The Astrophysical Journal, 583:L35–L38, 2003 January 20

DETECTION OF GAPS IN CIRCUMSTELLAR DISKS

J. Steinacker
Astrophysical Institute and University Observatory, University of Jena, Schillergässchen 2-3, D-07745 Jena, Germany; stein@astro.uni-jena.de

and

Th. Henning
Max-Planck-Institut für Astronomie, Königstuhl 17, D-69117 Heidelberg, Germany; henning@mpia-hd.mpg.de
Received 2002 October 26; accepted 2002 December 6; published 2002 December 17

ABSTRACT

We analyze the spectral appearance of gaps occurring in circumstellar disks possibly indicating the presence of a protoplanetary or planetary object. Based on the standard parameterized disk model, we explore the 10-parameter space of possible disk configurations and properties to identify the parameter ranges where the ratio of the continuum flux from disks without and with a gap is maximum. The exploration is performed with a Monte Carlo search; the maxima are found using a simulated annealing algorithm. The strongest influence on the spectra occurs for wavelengths ranging from 10 to 300 μm, with a maximum flux ratio of 1.5 for a single-planet gap and 2.5 for a double-planet gap, respectively. Analyzing the resulting spectra, we conclude that, investigating spectral energy distributions without spectral dust features, gaps typically caused by planets cannot be detected as a prominent feature.

Subject headings: accretion, accretion disks — circumstellar matter — planetary systems: formation — planetary systems: protoplanetary disks — planets and satellites: formation — radiative transfer

1. INTRODUCTION

With the increasing number of radial velocity detections of extrasolar planets[1] and resolved images of circumstellar disks around young stellar objects (McCaughrean, Stapelfeldt, & Close 2000), the question of how planets form from a disk is one of the key questions of current astrophysical research. Hydrodynamical simulations indicate that a planet in a disk may cause gaps, warps, or spirals in the disk distributions while interacting with it (Kley 1999, 2000; Bryden et al. 1999; d'Angelo, Henning, & Kley 2002). Therefore, detecting the signature of a planet in a circumstellar disk would reveal at which evolutionary state of star and disk the formation of planets occurs. For the nearest star-forming regions, direct imaging of circumstellar disks has been performed and will require a detailed radiative transfer modeling in order to analyze the observed images. A first prospective study dealing with gaps in disks was presented in Wolf et al. (2002). Using a three-dimensional hydrodynamical simulation of planet-disk interaction, they investigated if the gap of the calculated disk can be detected using the Very Large Telescope Interferometer or the Atacama Large Millimeter Array.

For most of the young stars, only an infrared or millimeter excess has been measured as indication of an accretion disk. Moreover, the variety and complex interplay of the many physical quantities to describe the circumstellar disk prohibit running realistic two- and three-dimensional radiative transfer programs for the calculation of all possible spectra. Nevertheless, only with a careful investigation of the wide parameter space, optimal parameters to maximize the impact of the gap on the spectral appearance can be determined.

In this Letter, we address the question whether for such disks density signatures from a planet-disk interaction can be observed. We focus on the most prominent feature, namely, a gap in the dust distribution, and investigate for which disk parameters the spectral energy distribution (SED) modification is maximum.

Applying the basic standard geometrically thin disk model used, e.g., by Weintraub, Sandell, & Duncan (1991), in § 2, we derive the optimal parameter sets to observe gaps in disks caused by a single planet and a two-planet system, respectively. The thin-disk spectral ratios are shown for the optimal parameters, and the findings are summarized and discussed in § 3.

2. PARAMETER SPACE EXPLORATION

2.1. *Gaps Caused by Single Planets*

The simplest analytical approach to describe a geometrically thin disk is given by Adams, Lada, & Shu (1988), including 10 free parameters. An extended model now widely used to fit SEDs was derived by Chiang & Goldreich (1997). They included an optically thin layer of superheated dust grains to account for emission features of dust, and hence, more free parameters. Even more parameters enter a detailed study of single disks using a multidimensional hydrodynamical (Kley, d'Angelo, & Henning 2001) and radiative transfer code (Steinacker et al. 2002).

To investigate for which parameter sets a detection of gaps in a disk is more likely, we start with the basic standard geometrically thin disk model having a parameter set that can be handled numerically. With this approximation, the spectral energy density of the disk at the wavelength λ at the distance d, inclined by the angle θ and extending from the radial coordinates r_1 to r_2, is given by

$$\lambda F_\lambda = \frac{2\pi \cos\theta}{d^2} \int_{r_1}^{r_2} \lambda B_\lambda(T)(1 - e^{-\tau_\lambda/\cos\theta}) 2\pi r\, dr, \qquad (1)$$

with specific flux F_λ, the Planck function $B_\lambda(T)$, the dust temperature T, and the optical depth τ_λ for rays through the plane (Adams et al. 1988; Thamm, Steinacker, & Henning 1994).

Assuming dust without specific spectral features, with a par-

[1] See, e.g., http://exoplanets.org/almanacframe.html.

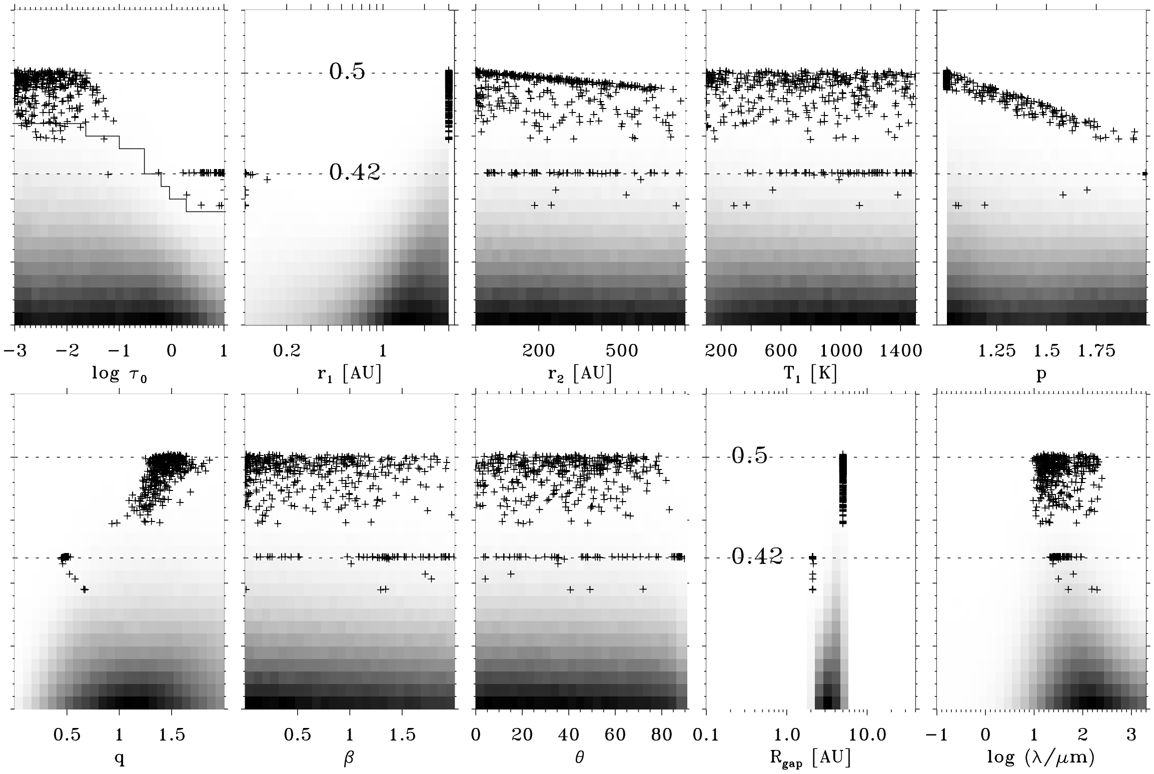

FIG. 1.—SED ratio $\mathcal{D} - 1$ for a disk without and with a gap caused by a planet as function of the free parameters optical depth, inner radius, outer radius, inner temperature, density gradient, temperature gradient, opacity gradient, inclination, gap radius, and wavelength, in the range 0.3–0.55. The gray shading indicates the number of MC attempts per parameter interval; the plus signs are parameter sets maximizing $\mathcal{D}$ obtained by SA maximization. The solid histogram marks the limit of the MC attempts.

ameterized dust temperature $T(r) = T_1\,(r/r_1)^{-q}$, a surface density of the disk $\Sigma(r) = \Sigma_1\,(r/r_1)^{-p}$, and a power-law opacity $\kappa_\lambda = \kappa_0\,(\lambda/\lambda_0)^{-\beta}$, the optical depth is $\tau_\lambda(r) = \tau_0(\lambda/\lambda_0)^{-\beta}(r/r_1)^{-p}$. The constants are the temperature at the inner radius $T_1 = T(r_1)$, the surface density $\Sigma_1 = \Sigma(r_1)$, the opacity κ_0 at the wavelength $\lambda_0 = 250\ \mu$m, and the optical depth $\tau_0 = \kappa_0\Sigma_1$ at r_1 and λ_0.

Parameterizing the density used in Wolf et al. (2002), we assume that the gap caused by a single planet occurs at $r = R_{\rm gap}$ with a radial Gaussian profile of the form

$$G_{\rm sp}(r) = 1 - \exp\left[-\left(\frac{r - R_{\rm gap}}{w}\right)^2\right] \qquad (2)$$

and width w of about 1 AU. There are two effects of the gap on the spectrum: the contribution of the dust in the gap will be missing, and the radiation transport will be altered in the gap region, changing the temperature. For the exploration of the parameter space, we neglect the second effect, which causes a small additional heating at the outer edge of the gap. Hence, only the density entering the optical depth is multiplied by $G_{\rm sp}$. The ratio of spectral energy densities $\mathcal{D} = \lambda F_\lambda/\lambda F_\lambda|_{\rm gap}$ for a disk without and with a gap yields $\mathcal{D} = f(\tau)/f(\tau_{\rm gap})$, with

$$f(\tau) = \int_{r_1}^{r_2} \frac{1 - e^{-\tau/\cos\theta}}{e^{hc/kT\lambda} - 1}\, r\, dr. \qquad (3)$$

In total, 10 free parameters enter the ratio $\mathcal{D}(\tau_0, r_1, r_2, T_1, p, q, \beta, \theta, R_{\rm gap}, \lambda)$. We are interested in the range of parameter sets for which the gap has a maximum impact on the spectrum, hence $\mathcal{D}$ is maximum.

We assume the following parameter ranges typical for circumstellar disks around low-mass young stellar objects. The inner radius r_1 is chosen between 10 stellar radii and 3 AU; the outer radius r_2 ranges from 100 to 1000 AU. For the gap radius, we allow values from $R_{\rm gap} = 0.1$ AU to the Pluto orbit of about 40 AU. The disk temperature at r_1 varies from 100 to 1500 K, where the upper limit corresponds to the sublimation temperature of the dust. We consider τ_0 to range from 10^{-3} to 10. The resulting dust masses of the disk cover the range 10^{-8} to $10^{-4}\ M_\odot$. We note that for very low mass disks, the planet-disk interaction may no longer lead to gaps or radiative pressure may force the dust to fill a possible gap. As surface density gradient, we allow the common values from $p = 1$ to 2, and 0 to 2 for the temperature gradient. The opacity power law may change from constant opacity to opacities with gradients of index -2. The inclination varies between face-on and edge-on, the wavelength range considered here from 0.1 to 2000 μm.

The results of our Monte Carlo (MC) analysis are shown in Figure 1 by plotting $\mathcal{D} - 1$ as a function of the 10 parameters for the very top of the 10^9 MC attempts, corresponding to about eight points per parameter. The plot shows the number of parameter sets gray-scaled (black for maximum number of parameter sets, white for no parameter set). The values are drawn from uniform distributions within each individual parameter range.

In addition, we determined the local maxima of the function $\mathcal{D} - 1$ to find the best parameter sets for observing a gap in a circumstellar disk. The search was performed using simulated annealing (SA), which has already been used successfully for other applications (Thamm et al. 1994; Steinacker, Thamm, & Maier 1996). The algorithm is well suited especially for an extrema search in a parameter space with a large number of free parameters. The plus signs in Figure 1 indicate the derived

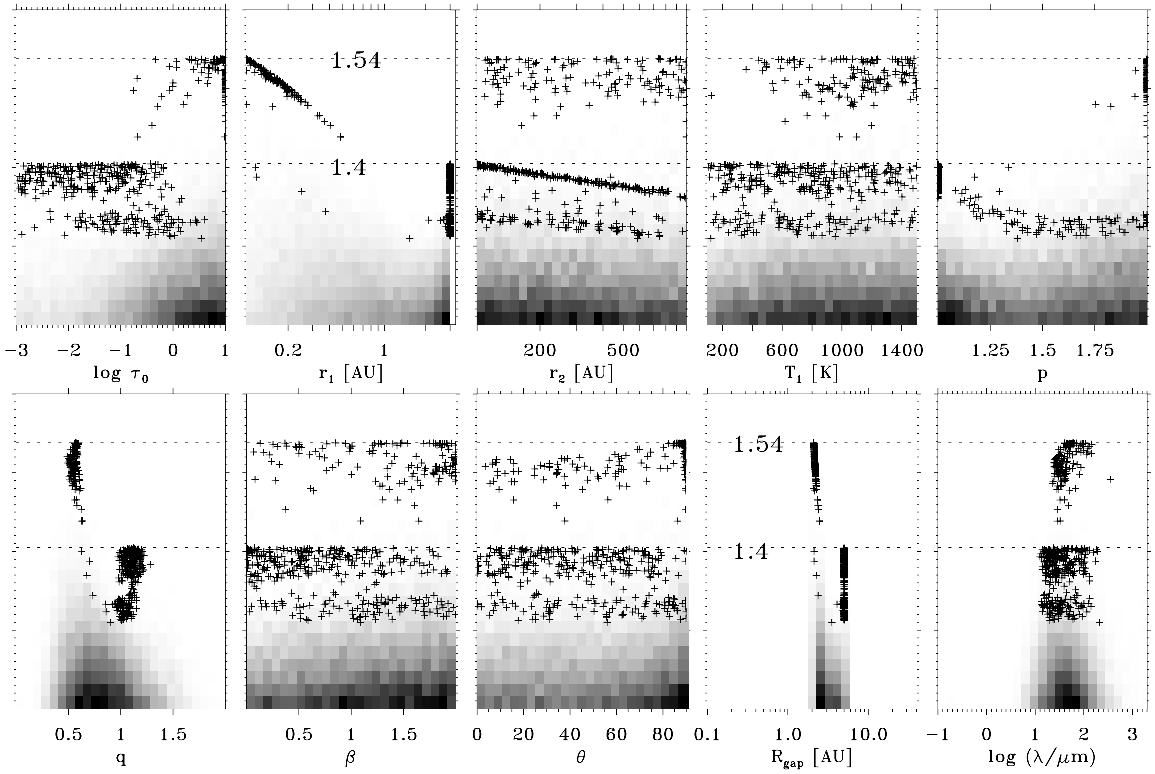

FIG. 2.—Same as Fig. 1, but in the range 1.2–1.45 and for a gap caused by two planets at 5 AU orbital distance

maxima from the SA search. They are in good agreement with the trend that already can be seen in the MC distribution and are above the highest MC values (*solid histogram*).

We proceed to explain the single panels of Figure 1. For high optical depth, the numerator of the integrand in equation (3) is about 1, and $\mathcal{D} - 1$ is small. Hence, the parameter sets with maximum $\mathcal{D} - 1$ are located in the optically thin regime $\tau_0 \ll 1$. The integrand in equation (3) in the optically thin approximation is

$$P = \frac{\tau_0 r}{\cos\theta}\left(\frac{\lambda}{\lambda_0}\right)^{-\beta}\left(\frac{r}{r_1}\right)^{-p}(e^{\alpha} - 1)^{-1}, \qquad (4)$$

with $\alpha = (hc/k\lambda T_1)(r/r_1)^q$. For small r, $P \propto r^{1-p-q}$, and for large r, $P \propto r^{1-p}\exp(-\alpha)$. As P decreases monotonically with r, the maximum flux contrast between the disk with and without a gap is achieved when the gap is located in the inner parts of the disk, where P is largest, and is smaller for the rest of the disk.

Moreover, the inner radius should be large to have most of the disk parts without a gap in the exponential part. Hence, the inner radius r_1 adjusts to the largest possible value of 3 AU, and the gap starts close to r_1. As we enforced $R_{gap} > r_1 + 2w$ to have the full gap being part of the disk, the maxima occur at $R_{gap} = 5$ AU. An increase of the outer radius r_2 will slightly increase the contribution from the rest of the disk and hence lower $\mathcal{D}$.

We discuss the two limiting cases of achieving the optically thin case $\tau/\cos\theta \ll 1$, which can be found as two distinct groups of maxima in Figure 1. If τ_0 is as small as 10^{-3}, β and θ are weakly constrained. As $\lambda/\lambda_0 < 1$ for most relevant wavelengths, β below 1.7 is favorable. For inclinations below 80°, $\cos\theta$ stays large enough to have $\tau/\cos\theta \ll 1$. The radial surface density distribution tends to be flat to have the largest contribution from the inner parts of the disk where the gap is located, yielding p near 1.

Optimal contrast between the spectra with and without a gap in the disk is achieved when the gap lies in the power-law part and the outer disk in the exponential part of equation (4). For small q, the turnover radius $r_{to} = r_1(kT_1\lambda/hc)^{1/q}$ is smaller than r_1, if $kT_1\lambda/hc < 1$. The q-values for the maximum $\mathcal{D}$-values are therefore greater than 1. For $q \approx 2$, r_{to} starts to exceed R_{gap}, decreasing $\mathcal{D}$. To have a turnover behind the gap, T_1, q, and λ adjust to have $hc(7/3)^q \approx \lambda k T_1$. Together with the upper limit of $T_1 = 1500$ K (where the dust sublimates), this determines the lower limit of λ for the maxima of $\mathcal{D}$ of around 10 μm.

The second group of maxima occurs for $\tau_0 \geq 1$, with a lower $\mathcal{D}$ of about 1.4. To reach $\tau < 1$, nevertheless, p has to be maximum as $r > r_1$, and the left upper panel of Figure 1 gives $p = 2$ for this group of maxima. Moreover, the optical depth is reduced when decreasing r_1, and the second group has $r_1 = 0.1$ AU. The gap location is shifted with r_1 toward the inner parts, yielding $R_{gap} > 2.1$ AU, as $R_{gap} > r_1 + 2w$. The strong decrease of τ by the $(r/r_1)^{-(1/q)}$ term relaxes the conditions for β and θ, so they are spread over the entire parameter range. As q is larger now, T_1 and λ are increased to guarantee that the turnover point is still located behind the gap.

We conclude that within the simple geometrically thin disk model for SEDs without spectral dust features, gaps typically caused by a single planet can be seen best for small optical depth, larger inner radii, a surface density gradient of around −1, a temperature gradient of about −1.5, gaps as far out as 5 AU, and at wavelengths between 10 and 300 μm. Outer radius, inner temperature, opacity gradient, and inclination are ambiguous in their influence on the spectral gap appearance and do not allow for a clear range determination. For circumbinary disks, large inner radii can be expected owing to tidal forces, favoring the detection of potential single-planet gaps.

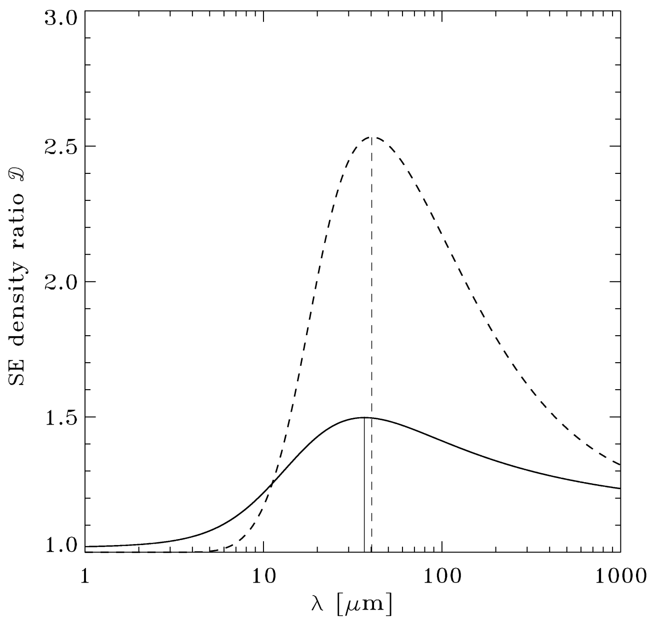

FIG. 3.—$\mathcal{D}$ as a function of the wavelength λ for the case of a gap caused by a single planet (*solid line*) and by two planets (*dashed line*). The vertical lines indicate the maximum λ found from the SA maximization.

The findings are valid only for the case when the disk mass is sufficiently large so that the disk-planet interaction yields to the formation of the gap as found in the quoted hydrodynamical simulations. For small disk masses and luminous central stars, also effects like radiation pressure might influence the formation of a gap.

2.2. *Gaps Caused by Two Planets*

If more than one planet interacts with the disk, larger gaps are found to open in hydrodynamical simulations (Bryden et al. 2000), extending between the orbits of the planets. We assume here a two-planet system following Kley (2000) and parameterize the gap by modifying equation (2) as $G_{\rm dp} = G_{\rm sp}\,[H(R_{\rm gap} - r) + H(r - R_{\rm gap} - 5\ {\rm AU})]$ with the Heaviside function H. The distance of the planet orbits is another free parameter, but we discuss here the case of a wide distance as a possible upper limit only. Owing to the weak influence of the temperature, simultaneous modification of the temperature at the outer edge of the gap is neglected. The results given in Figure 2 are similar to the single-planet case, with a stronger deviation from the gapless disk spectral energy yielding to $\mathcal{D} < 2.6$. Prominently, the two maxima groups distinguished in § 2.1 are present for wider gaps, but the group corresponding to small τ_0 reaches values of $\mathcal{D} = 2.4$ while the high-τ_0 maxima go up to $\mathcal{D} = 2.54$. This change is caused by the fact that with a wider gap, the optimum is no longer to have the gap end at the turnover point from power-law integrand to exponential integrand, as the gap can cover all parts of power-law decrease.

To sum up, for a typical double-planet gap in a disk described by the thin-disk model for SEDs, we find a maximum factor of 2.5 in the spectral energy ratio for a disk with and without a gap when no spectral dust features are present. The maximum occurs for high optical depth, small inner disk radii, surface density exponents of about −1, temperature exponents of −0.5, inner gap radii of a few AU, and wavelengths ranging from 10 to 300 μm.

3. DISCUSSION AND CONCLUSIONS

In Figure 3, the maximal SED ratios of the disks with and without the gap are shown. The thick solid line corresponds to the case of one planet, and the vertical line indicates the optimal wavelength derived by the SA maximization, in agreement with the maximum of the graph. The dashed line shows $\mathcal{D}$ for the wider two-planet gap. The gap feature extends over 3 orders of wavelength, smeared out by the Planck function of the radially dependent temperatures. For unknown disk parameters, it will be impossible to distinguish this feature from variations in the disk and dust parameters, even if some of the parameters like inclination are determined independently. Moreover, the error bars in the observed fluxes will further hinder the gap identification.

A variety of spectra of T Tauri stars show solid-state features like the amorphous silicate features at 10 and 20 μm (Mathis 1990) or the polycyclic aromatic hydrocarbon features at 3.3 and 6.2 μm (Waelkens et al. 1996). The features are confined to a small wavelength region, but they also introduce more parameters to describe them and to model the optically thin layer above the thick disk or a contribution from optically thin emission in the disk (Chiang & Goldreich 1999). But even in this case, it will be hard to distinguish whether the absence of a feature arises from the possible presence of a gap or the absence of this specific dust material in the disk. The only exception might be the combined 10 and 20 μm feature. The detection of a spectrum revealing just one of the amorphous silicate features might hint toward a depression in the radial surface density when the disk parameters are favorable for the detection. We refer to a forthcoming paper for the detailed investigation of this problem including a high number of free parameters.

REFERENCES

Adams, F. C., Lada, C. J., & Shu, F. H. 1988, ApJ, 326, 865
Bryden, G., Chen, X., Lin, D. N. C., Nelson, R. P., & Papaloizou, C. B. 1999, ApJ, 514, 344
Bryden, G., Różyczka, M., Lin, D. N. C., & Bodenheimer, P. 2000, ApJ, 540, 1091
Chiang, E. I., & Goldreich, P. 1997, ApJ, 490, 368
———. 1999, ApJ, 519, 279
d’Angelo, G., Henning, Th., & Kley, W. 2002, A&A, 385, 647
Kley, W. 1999, MNRAS, 303, 696
———. 2000, MNRAS, 313, L47
Kley, W., d’Angelo, G., & Henning, Th. 2001, ApJ, 547, 457
Mathis, J. M. 1990, ARA&A, 28, 37
McCaughrean, M. J., Stapelfeldt, K. R., & Close, L. M. 2000, in Protostars and Planets IV, ed. V. Mannings, A. P. Boss, & S. S. Russell (Tuscon: Univ. Arizona Press), 485
Steinacker, J., Henning, Th., Bacmann, A., & Semenov, D. 2002, A&A, in press
Steinacker, J., Thamm, E., & Maier, U. 1996, J. Quant. Spectrosc. Radiat. Transfer, 56, 97
Thamm, E., Steinacker, J., & Henning, Th. 1994, A&A, 287, 493
Waelkens, C., et al. 1996, A&A, 315, L245
Weintraub, D. A., Sandell, G., & Duncan, W. D. 1991, ApJ, 382, 270
Wolf, S., Gueth, F., Henning, Th., & Kley, W. 2002, ApJ, 566, L97